Superconductivity of single unit cell FeSe/SrTiO$_3$(001): Substrate-surface superstructure dependence

Tomoaki Tanaka, Kenta Akiyama, Ryo Yoshino, and Toru Hirahara[*]

Department of Physics, Tokyo Institute of Technology, Tokyo 152-8551, Japan

We report the relationship between the surface superstructure of SrTiO$_3$(001) (STO) substrates and the superconducting properties of single unit cell (1-UC) FeSe films using scanning tunneling microscopy/spectroscopy (STM/STS). Under reflection high-energy-electron diffraction observation, we controlled the periodicity of the STO surface to 2×1 and $\sqrt{2} \times \sqrt{2}$ and grew high-quality FeSe films. We found that the substrate periodicity can be imaged through the 1-UC FeSe from high-resolution STM observations and obtained clear evidence that the superconducting gap size depends on the surface periodicity (10–15 meV on 2×1, 12–17 meV on $\sqrt{2} \times \sqrt{2}$, and 9–13 meV for 2×1 domains on the $\sqrt{2} \times \sqrt{2}$ surface). Our results strongly suggest the important role of the film/substrate interface on high-temperature superconductivity.

Iron-based superconductors have attracted a lot of attention [1] and FeSe is believed to be useful in exploring unconventional mechanisms due to its simple crystal structure. Furthermore, a single unit cell (1-UC) FeSe film on a SrTiO$_3$(001) (STO) substrate was reported to exhibit a higher superconducting transition temperature ($T_c \sim 60$–109 K [2–4]) than that of the bulk (8 K) [5] and has been extensively investigated. The film/substrate interface is thought to be important in terms of carrier doping by oxygen vacancies [6] and band bending [7], or optical phonons [8].

On the STO surface which is at the interface between FeSe and STO, various superstructures such as 1×1, 2×1, $c(4 \times 2)$, $c(6 \times 2)$ [9], $c(4 \times 4)$ [10], $\sqrt{5} \times \sqrt{5}$ [11], $\sqrt{13} \times \sqrt{13}$ [12], and $\sqrt{2} \times \sqrt{2}$ [13] have been reported to exist. This is due to the difference in the oxygen deficiencies [14], the off stoichiometry of Sr or Ti [15], or different terminations (TiO$_2$ or SrO) [13]. Thus one can imagine that the STO surface superstructure should influence the superconducting properties of the 1-UC FeSe. But there have been only few studies that have examined how the difference of surface periodicity influences the 1-UC FeSe [16]. Especially, no experimental work has systematically reported the difference in superconductivity for various superstructures. The scattering in T_c reported in the literature [2–4] may originate from this difference at the surface that has yet to be investigated seriously.

Therefore, in the present Rapid Communication, we aimed to clarify the relationship between the surface superstructure of the STO substrate and the superconducting properties of 1-UC FeSe. With scanning tunneling microscope/spectroscopy (STM/STS), we measured the superconducting properties of a 1-UC FeSe film grown on surfaces with controlled periodicity (2×1 and $\sqrt{2} \times \sqrt{2}$). Regions that were 0.2 nm higher than the usual domains existed for the 1-UC FeSe films formed on the STO-$\sqrt{2} \times \sqrt{2}$ substrate. These domains surprisingly

showed a 2×1 periodicity. We found clear evidence that the superconducting gap size depends on the surface periodicity (10–15 meV on 2×1, 12–17 meV on $\sqrt{2} \times \sqrt{2}$, and 9–13 meV for 2×1 domains on the $\sqrt{2} \times \sqrt{2}$ surface).

Nb-doped STO(001) (Shinkosha, 0.5 wt. %) substrates were used in this study. After degassing at 500 °C for more than 3 h, they were heated at 1000 °C for 30 min under Se flux (Se etching) [2]. Then they were annealed at various temperatures (500–1000 °C) for 30 min. The brightest reflection high-energy-electron diffraction (RHEED) patterns were found at 950 °C for STO-2×1, whereas it was at 710 °C for STO-$\sqrt{2} \times \sqrt{2}$. Figures 1(a) and 1(b) show the RHEED patterns after the above procedure. The inset shows the features near the zeroth Laue zone. All the spots are sharp, which shows that the substrate is flat and the surface superstructure is controlled at the atomic level. The spots in the red, blue, and green circles indicate 1×1, 2×1, and $\sqrt{2} \times \sqrt{2}$, periodicity, respectively. The red dashed line represents the straight line connecting a 1×1 spot in the zeroth Laue zone with it in the first Laue zone. The 2×1 spots exist on the zeroth, first, and 1/2 Laue zones and the spots on the 1/2 Laue zone are aligned on the red line in Fig. 1(a). On the other hand, the $\sqrt{2} \times \sqrt{2}$ spots exist only on the 1/2 Laue zone, and there are no spots on the red line in Fig. 1(b).

The FeSe films were grown by coevaporating Fe (99.5%) and Se (99.999%) with a flux ratio of $\sim$1 : 10 at a substrate temperature of 480 °C, followed by annealing at the same temperature for 5 min or 1 h. The RHEED patterns after depositing FeSe on each substrate are shown in Figs. 1(c) and 1(d). Both show the streak patterns of 1×1 FeSe.

After the sample preparation, they were transferred to a STM/STS system (Unisoku, USM1500). The measurements were performed at 5 K with a PtIr tip. The dI/dV spectra were acquired using the lock-in technique with a bias modulation of 1 mV at 1093 Hz.

Figure 2(a) shows the topographic image of FeSe films on STO-2×1 after annealing for 1 h. Figure 2(b) shows the line profile along the blue arrow in Fig. 2(a). The inset is the

*hirahara@phys.titech.ac.jp

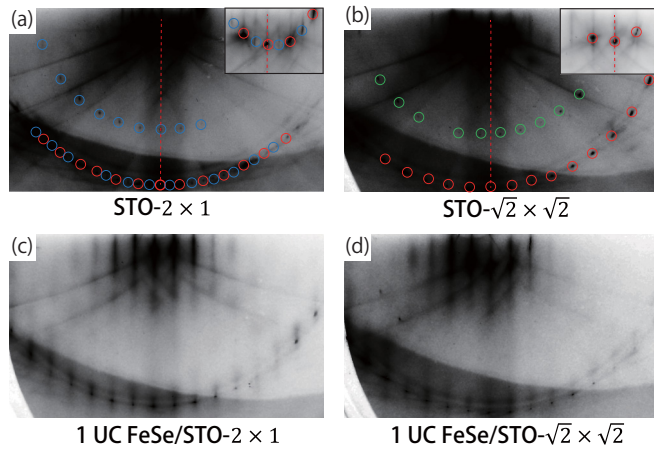FIG. 1. (a), (b) RHEED patterns of STO (001)-2×1 and $\sqrt{2} \times \sqrt{2}$ obtained after annealing at 950 and 710 °C for 30 min, respectively. The insets show the zeroth Laue zones of different contrast. The spots in the red, blue, and green circles indicate the 1×1, 2×1, and $\sqrt{2} \times \sqrt{2}$ spots, respectively. The red dashed lines in (a) and (b) represent straight lines connecting a 1×1 spot in the zeroth Laue zone with that in the first Laue zone. (c), (d) RHEED patterns of 1-UC FeSe deposited on (a) and (b), respectively. Electrons are incident from the [100] direction.

estimated surface morphology from the reported height of the FeSe (0.56 nm) and that of the step height of STO (0.39 nm). Figure S1 shows the topographic image of substrate STO-2×1, in which only ~0.4-nm steps are found [17]. It suggests

that 1-UC FeSe grows atomically flat on the STO, and 2-UC FeSe grows along the substrate step edges. A comparison between Figs. 2(a) and 2(b) and the data for the samples annealed just for 5 min [Figs. S2(a) and S2(b)] shows that the annealing time has little influence on the surface morphology.

Figure 2(c) is an enlarged topographic image of the 1-UC FeSe, and there are regions that show a different brightness. Figures 2(d) and 2(e) are atomic-resolution images obtained in the bright and dark regions, respectively. Figure 2(d) shows that the protrusions are lined up in a 1×1 periodicity (black square). They are likely Se atoms [2]. This is also clear from the fast Fourier transform (FFT) image shown in the inset. On the other hand, in Fig. 2(e) measured in the dark region, a 2×1 periodicity (blue rectangle) was also observed, as clearly indicated in the FFT image. This corresponds to the fact that the periodicity of the bright and dark atomic lines in Fig. 2(e) is twice the lattice constant (see the blue arrows). A stripe structure with the 2×1 periodicity in the topographic image of 1-UC FeSe has been reported [18], and the origin is suggested as the substrate electronic structure due to oxygen defects in the TiO$_2$-terminated STO substrate [6]. The 2×1 periodicity in Fig. 2(e) is slightly different from this stripe structure, but this should also reflect the electronic structure of the surface because 1-UC FeSe and STO strongly couple [18] and the 2-UC film only shows 1×1 periodicity (Fig. S3).

Figure 2(f) shows the averaged STS spectra measured in the bright and dark regions. A superconducting gap (Δ) is observed in both of them. To quantitatively estimate Δ, a normalization procedure was carried out using the extrapolation method [19] (Fig. S4). Δ, the position of the quasiparticle
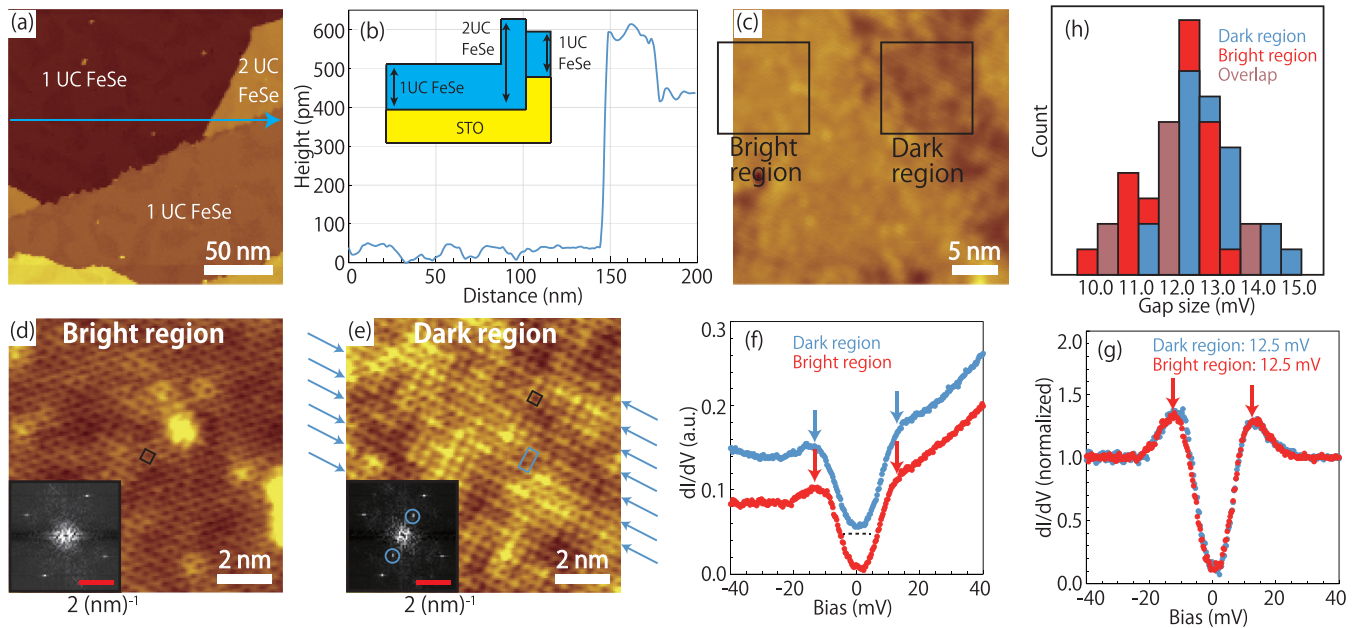

FIG. 2. (a) Topographic image of a FeSe on STO (001)-2×1 after annealing at 480 °C for 1 h (200 nm × 200 nm, 1.99 V, 296 pA). (b) Line profile along the blue arrow in (a). The inset shows the surface morphology. (c) Enlarged topographic image of 1-UC FeSe on STO (30 nm × 30 nm, 0.99 V, 295 pA). (d), (e) Atomically resolved images obtained in the bright and dark regions in (c), respectively (10 nm × 10 nm, 47 mV, 82 pA). The black and blue squares denote the 1×1 and 2×1 unit cells, respectively. The insets show FFT transformed images. (f) dI/dV spectra taken in the bright and bark regions (48 mV, 83 pA). (g) The dI/dV spectra normalized by the background obtained with the extrapolated method. (h) Statistical analysis of the distribution of the gap measured in the two regions (140 STS spectra were used).
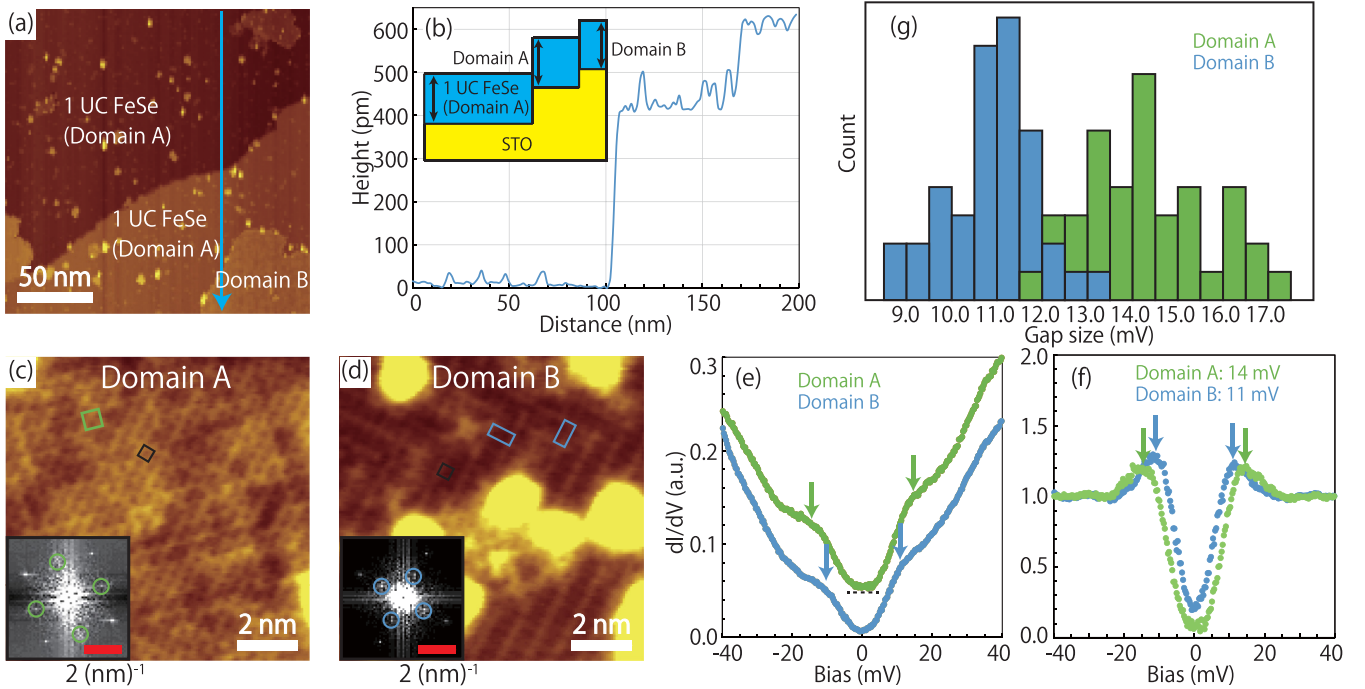
FIG. 3. (a) Topographic image of a FeSe on STO(001)-$\sqrt{2} \times \sqrt{2}$ after annealing at 480 °C for 5 min (200 nm × 200 nm, 0.99 V, 294 pA). (b) Line profile along the blue arrow in (a). The inset shows the surface morphology. (c), (d) Atomically resolved images obtained in domains A and B, respectively [10 nm × 10 nm, (c) −47 mV, 81 pA, (d) 45 mV, 82 pA]. The black, blue, and green squares denote the 1 × 1, 2 × 1, and $\sqrt{2} \times \sqrt{2}$ unit cells, respectively. The insets show FFT transformed images. (e) dI/dV spectra taken in domains A and B (46 mV, 81 pA). (f) The dI/dV spectra normalized by the background obtained by the extrapolated method. (g) Statistical analysis of the distribution of the gap measured in the two domains (140 STS spectra were used).

peak, was 12.5 meV in the both the bright and dark regions [Fig. 2(g)]. Figure 2(h) shows the statistical analysis of the distribution of Δ (about 140 spectra for each region used). It shows the peak is around 12.5 meV for both regions, and we conclude that the superconducting gap of 1-UC FeSe/STO(001)-2 × 1 is 12.5 ± 2.5 meV.

We note that neither atomic-resolution topographic images nor the gap were observed for the 5-min annealed sample (Fig. S2). It was reported that the superconductivity in FeSe/STO develops by an increase in annealing time, which makes the excess Se atoms at the interface disappear [20]. Our observation is in agreement with this. On the other hand, for the 2-UC FeSe, there was no difference between samples with different annealing times (Fig. S3). Thus this really shows that the interface is important for this 1-UC FeSe/STO system.

Next, we turn to FeSe films grown on STO(001)-$\sqrt{2} \times \sqrt{2}$. Figure 3(a) shows the topographic image of a FeSe thin film on STO-$\sqrt{2} \times \sqrt{2}$ after annealing for 5 min. One can see that 1-UC FeSe films also grow atomically flat on the STO-$\sqrt{2} \times \sqrt{2}$, but with slightly more bright protrusions. However, one notices a more significant difference. Figure 3(b) is a line profile along the blue arrow in Fig. 3(a). One can find flat domains that are not at the step edges but are 0.2 nm higher than the usual 1-UC FeSe and this seems to be different from the 2-UC FeSe (Fig. S5). In the following, to distinguish these domains, we will refer to the usual 1-UC FeSe as domain A and the 0.2-nm higher domain as domain B. A schematic drawing of the surface morphology that corresponds to the blue arrow in Fig. 3(a) is shown in the inset in Fig. 3(b).

Figures 3(c) and 3(d) show the atomically resolved topographic images obtained in domains A and B, respectively. In domain A, a $\sqrt{2} \times \sqrt{2}$ periodicity (green square) was observed, whereas in domain B, a 2 × 1 periodicity (blue rectangle) was obtained. These periodicities were also confirmed in the FFT images shown in the insets. On the other hand, as shown in Fig. S5(c), the 2-UC FeSe shows only 1 × 1 periodicity. This strongly suggests that domains A and B are both 1-UC FeSe and the electronic periodicity of the STO surface superstructure is observed through the FeSe film similar to what is shown in Figs. 2(d) and 2(e).

To investigate the origin of domain B, we have performed STM measurements on the pristine STO-$\sqrt{2} \times \sqrt{2}$ surface [Fig. S6(a)]. Most steps are ∼0.4 nm high, but there is a domain with a 0.1-nm height difference. This is different from that between domains A and B. Furthermore, the ratio of this domain inside the sample (∼1.7% among the four 600 × 600 nm² images) is smaller than that of domain B (∼12.5%). Therefore, we think domain B was formed during FeSe deposition [21].

Next, we measured the STS spectra for these domains as shown in Fig. 3(e). They show spatially averaged curves measured on the same sample (refer to Fig. S7 for position-dependent STS curves). One can clearly see that both domains A and B show superconductivity. This suggests that there is no excess Se at the interface after only 5 min of annealing, unlike the case of 1-UC FeSe/STO-2 × 1, and shows that the surface superstructure of STO changes the amount of Se atoms intercalated during FeSe film growth (after annealing

for 1 h, the quasiparticle peaks become weak with the increase in the number of bright protrusions). The STS spectrum of the 2-UC FeSe shown in Fig. S5(d) is similar to what it shown in Fig. S3(b) and previous studies. This reconfirms that only the first UC is strongly coupled to STO and also supports that domains A and B are both 1-UC FeSe.

Figure 3(f) shows the normalized STS spectra. The superconducting gap size is 14 and 11 meV for domains A and B, respectively. One can also notice that the zero bias conductance of domain B does not fall to zero in Fig. 3(f). The origin of this is unclear at the moment (see also Fig. S8). Figure 3(g) shows the distribution of the superconducting gap (about 140 spectra for each domain). It shows Δ is 14.5 ± 2.5 meV in domain A and 11.0 ± 2.0 meV in domain B. Thus there is a systematic difference between domains A and B that exists on the same sample. Therefore we have obtained clear evidence that the superconducting gap of 1-UC FeSe depends on the STO substrate-surface superstructure.

Let us briefly consider the origin of the height difference of 0.2 nm between domains A and B. As mentioned above, domains A and B are both 1-UC FeSe, and the height difference is probably caused by the difference in the STO surface superstructures. Since the height difference between SrO and TiO_2 terminations is reported as 0.19 nm [22] and that between the double- and single-layer TiO_2 is reported as 244 ± 80 pm [20], the value of 0.2 nm can be simply assumed to be due to an additional SrO or TiO_2 layer. STO-2×1 is known to be TiO_2 terminated, and models based on double-TiO_2-layer termination [20,23,24] or single-TiO_2-layer termination [10] have been proposed, although there may be other possibilities [25]. On the other hand, STO-$\sqrt{2} \times \sqrt{2}$ is experimentally shown to be SrO terminated by annealing in atmosphere [13], while a double-TiO_2-layer termination is reported by theoretical calculations [23]. In addition to the difference of the surface termination, the proposed models for the STO surface can actually be quite complex [6,10,25–27]. Thus structural studies at atomic precision with low-energy electron

diffraction (LEED-IV) or surface x-ray diffraction are needed to make a definite conclusion. Such studies should also help in identifying why there is a difference in the superconducting gap size.

One should also note that even though the dark region in Fig. 2(e) and domain B in 3(d) are measured at nearly the same conditions and both show 2×1 periodicity, the atomic-resolution images look very different (see also Fig. S9). The domain sizes are also significantly different as Fig. 2(e) is a single domain, whereas in Fig. 3(d), one can see the two domains rotated by $90°$ to each other exist closely. And finally the superconducting gap size is slightly different (10–15 meV for the dark region and 9–13 meV on domain B). These facts strongly suggest that although the periodicity is the same, the electronic structure (and presumably the atomic structure) should be different between the two. Thus one should also keep in mind that the actual surface structure can be different even when the periodicity is the same.

In summary, we investigated the superconducting properties of 1-UC FeSe on controlled surface superstructures of STO(001). We were able to observe atomic-resolution images and identify the substrate-surface periodicity through the 1-UC FeSe film. We found clear evidence that the superconducting gap size depends on the surface superstructure. Our results suggest that the superconducting transition temperature can be controlled by the surface superstructure of the substrate and, moreover, by investigating other surfaces as well as their structures at the atomic level, it may be possible to clarify details of the influence of electron doping and optical phonons, and hopefully realize even higher T_c.

[1] Y. Kamihara, H. Hiramatsu, M. Hirano, R. Kawamura, H. Yanagi, T. Kamiya, and H. Hosono, J. Am. Chem. Soc. **128**, 10012 (2006).

[2] Q.-Y. Wang, Z. Li, W.-H. Zhang, Z.-C. Zhang, J.-S. Zhang, W. Li, H. Ding, Y.-B. Ou, P. Deng, K. Vhang, J. Wen, C.-L. Song, K. He, J.-F. Jia, S.-H. Ji, Y.-Y. Wang, X. Chen, X.-C. Ma, and Q.-C. Xue, Chin. Phys. Lett. **29**, 037402 (2012).

[3] S. Tan, Y. Zhang, M. Xia, Z. Ye, F. Chen, X. Xie, R. Peng, D. Xu, Q. Fan, H. Xu, J. Jiang, T. Zhang, X. Lai, T. Xiang, J. Hu, B. Xie, and D. Feng, Nat. Mater. **12**, 634 (2013).

[4] J.-F. Ge, Z.-L. Liu, C. Liu, C.-L. Gao, D. Zian, Q.-K. Xue, Y. Liu, and J.-F. Jia, Nat. Mater. **14**, 285 (2014).

[5] F.-C. Hsu, J.-Y. Luo, K.-W. Yeh, T.-K. Chen, T.-W. Huang, P. M. Wu, Y.-C. Lee, Y.-L. Huang, Y.-Y. Chu, D.-C. Yan, and M.-K. Wu, Proc. Natl. Acad. Sci. USA **105**, 14262 (2008).

[6] J. Bang, Z. Li, Y. Y. Sun, A. Samanta, Y. Y. Zhang, W. Zhang, L. Wang, X. Chen, X. Ma, Q.-K. Xue, and S. B. Zhang, Phys. Rev. B **87**, 220503(R) (2013).

[7] H. Ding, Y.-F. Lv, K. Zhao, W. L. Wang, L. Wang, C.-L. Song, X. Chen, X.-C. Ma, and Q.-K. Xue, Phys. Rev. Lett. **117**, 067001 (2016).

[8] J. J. Lee, F. T. Schmitt, R. G. Moore, S. Johnston, Y.-T. Cui, W. Li, M. Yi, Z. K. Liu, M. Hashimoto, Y. Zhang, D. H. Lu, T. P. Devereaux, D.-H. Lee, and Z.-X. Shen, Nature (London) **515**, 245 (2014).

[9] Q. D. Jiang and J. Zegenhagen, Surf. Sci. **425**, 343 (1999).

[10] M. R. Castell, Surf. Sci. **505**, 1 (2002).

[11] T. Kubo and H. Nozoye, Surf. Sci. **542**, 177 (2003).

[12] M. Naito and H. Sato, Physica C **229**, 1 (1994).

[13] S. Ogawa, K. Kato, N. Nagatsuka, S. Ogura, and K. Fukutani, Phys. Rev. B **96**, 085303 (2017).

[14] R. Shimizu, K. Iwaya, T. Ohsawa, S. Shiraki, T. Hasegawa, T. Hashizume, and T. Hitosugi, Appl. Phys. Lett. **100**, 263106 (2012).

[15] J. Ciston, H. G. Brown, A. J. D Alfonso, P. Koirala, C. Ophus, Y. Lin, Y. Suzuki, H. Inada, Y. Zhu, L. J. Allen, and L. D. Marks, Nat. Commun. **6**, 7358 (2015).

[16] K. Zou, S. Mandal, S. D. Albright, R. Peng, Y. Pu, D. Kumah, C. Lau, G. H. Simon, O. E. Dagdeviren, X. He, I. Bozovic, U. D. Schwarz, E. I. Altman, D. Feng, F. J. Walker, S. Ismail-Beigi, and C. H. Ahn, Phys. Rev. B **93**, 180506 (2016).

[17] See Supplemental Material at http://link.aps.org/supplemental/10.1103/PhysRevB.98.121410 for additional information about the contents of this Rapid Communication that shows complementary data of STM/STS measurements taken at different sample conditions and also a detailed description about the analysis method.

[18] Z. Li, J.-P. Peng, H.-M. Zhang, W.-H. Zhang, H. Ding, P. Deng, K. Chang, C.-L. Song, S.-H. Ji, L. Wang, K. He, X. Chen, Q.-K. Xue, and X.-C. Ma, J. Phys.: Condens. Matter **26**, 265002 (2014).

[19] M. A. Ivan, R. Christophe, E. Andreas. W. Eric, R. Bernard, G. Jean-Yves, K. Kadowaki, and O. Fischer, J. Electron Spectrosc. Relat. Phenom. **109**, 147 (2000).

[20] F. Li, Q. Zhang, C. Tang, C. Liu, J. Shi, C. Nie, G. Zhou, Z. Li, W. Zhang, C. L. Song, K. He, S. Ji, S. Zhang, L. Gu, L. Wang, X.-C. Ma, and Q.-K. Xue, 2D Mater. **3**, 024002 (2016).

[21] The 2×1 periodicity was not observed with RHEED for the substrate as shown in Fig. 1(b). This also suggests that domain B is probably formed during the FeSe film growth.

[22] T. Hikita, T. Hanada, M. Kudo, and M. Kawai, Surf. Sci. **287–288**, 377 (1993).

[23] W. Oliver, A. Mark, E. Natasha, P. R. Kenneth, E. E. Donald, and M. D. Laurence, Surf. Sci. **573**, 446 (2004).

[24] J. Wang, M. Fu, X. S. Wu, and D. Bai, J. Appl. Phys. **105**, 083526 (2009).

[25] M. Xu, X. Songa, and H. Wang, Phys. Chem. Chem. Phys. **19**, 7964 (2017).

[26] S. Gerhold, Z. Wang, M. Schmid, and U. Diebold, Surf. Sci. **621**, L1 (2014).

[27] T. Kubo, H. Orita, and H. Nozoye, Phys. Chem. Chem. Phys. **13**, 16516 (2011).